Dynamic structure of dense krypton gas

P. A. Egelstaff
Physics Department, University of Guelph, Ontario, Canada N1G 2W1

J. J. Salacuse
National Bureau of Standards, Washington, D.C., 20234

W. Schommers
Kernforschungszentrum Karlsruhe, Institut für Nucleare Festkörperphysik, D-7500 Karlsruhe, West Germany

J. Ram
Banaras Hindu University, Varanasi, India 221005

(Received 20 January 1984)

We have made molecular-dynamics computer simulations of dense krypton gas (10.6×10^{27} atoms/m^3 and 296 K) using reasonably realistic pair potentials. Comparisons are made with the recent experimental data [P. A. Egelstaff *et al.*, Phys. Rev. A **27**, 1106 (1983)] for the dynamic structure factor $S(q,\omega)$ over the range $0.4<q<3.0$ Å^{-1}. For $q<1.6$ Å^{-1} the influence of the attractive part of the potential is important and shorter-ranged many-body forces are found to play a role. Additional (less significant on a relative scale) effects are found in the region $q\sim2.7$ Å^{-1}. Some suggestions for future work are made.

I. INTRODUCTION

A series of experiments on the dynamic structure factor of dense krypton gas have been published,[1] and the data compared to hard-sphere-fluid results. It was found that if the momentum transfer ($\hbar q$) was greater than $q=2\pi/\sigma$ (where σ is an equivalent hard-sphere diameter), the experimental and hard-sphere results were quite similar. But for $q<2\pi/\sigma$ there were significant differences, which may have been due to the role played by the attractive part of the potential in multiple collision processes. To investigate these questions further and to study the role of many-body forces in dynamic phenomena, we have made molecular-dynamics (MD) calculations using a realistic krypton pair potential,[2,3] and compared them to the experimental krypton data.

In Sec. II we describe two series of MD calculations using 250 and 500 particles, and in Sec. III the comparisons are made and discussed. Although a more precise and extensive set of MD calculations would be useful, we feel that the initial comparisons made here are very informative and provide a good foundation for future work.

II. MOLECULAR-DYNAMICS CALCULATIONS

The Fourier transform of the microscopic number density of a system with N krypton atoms having positions $\vec{r}_j(t)$, $j=1,\ldots,N$, is given by

$$\rho_q(t)=\frac{1}{\sqrt{N}}\sum_{j=1}^{N}\exp[i\vec{q}\cdot\vec{r}_j(t)]\ . \tag{1}$$

To describe density fluctuations, the correlation function $I(q,t)$ (intermediate scattering function) is of interest:

$$I(q,t)=\langle\rho_{-q}(0)\rho_q(t)\rangle\ . \tag{2}$$

From this we obtain the coherent scattering law $S(q,\omega)$ by

$$S(q,\omega)=\frac{1}{2\pi}\int_{-\infty}^{\infty}I(q,t)\exp(i\omega t)dt\ . \tag{3}$$

For our model system the nonzero components are those for which

$$\vec{q}=\frac{2\pi}{L}(l_1,l_2,l_3)\ , \tag{4}$$

where l_1, l_2, and l_3 are positive and negative integers.

For a given wave vector $\vec{q}$ we can calculate $I(\vec{q},t)$ on the basis of the molecular-dynamically determined positions $\vec{r}_i(t)$ of the N atoms as a function of time. Then, for a suitably chosen Δq, by adding the results for all q in a shell given by the magnitude q, $q+dq$, and dividing by the number of vectors $\vec{q}$ in the shell, we get $I(q,t)$. Clearly, for small values of q this averaging will be statistically less satisfactory than for large values of q.

Series I calculations were done at Cornell University on a Floating Point Systems' Array Processor, model 190L with an IBM 370/168 computer used as a host machine. The MD simulation was carried out for 256 particles in a box with periodic boundary conditions and interacting via an Aziz[2] pair potential with a diameter σ and a well depth ϵ/k, of 3.591 Å and 170 K, respectively (this is the same σ as the Barker[3] potential and about 85% of its well depth). A reduced density $\rho^*(=\rho\sigma^3)$ of 0.4955 and a (required) reduced temperature $T^*(=kT/\epsilon)$ of 1.747 define the state point of the simulation. Finally, the interaction potential was modified by applying a cutoff distance of 2.5σ, and a time step (associated with the iterative solu-

tion of the classical equations of motion) of 2.765×10^{-15} sec was used. Two simulations of equal length were actually carried out. The first, MDA, from 0 to 10000 time steps was followed (continued) by MDB from 10000 to 20000 time steps. Essentially both simulations resulted in an energy conservation of $\Delta E^*/\langle E^*\rangle=0.0011$, with E^* $(=E/\epsilon)$ being the total reduced kinetic energy of the system and an average temperature $\langle T^*\rangle=1.7485$ ±0.036: to achieve this velocity rescaling was used during equilibration. The simulation ran at a rate of approximately 1900 time steps per hour, and the location or coordinates of each of the 256 particles were saved every 5 time steps. The particle coordinates resulting from this simulation were then processed to obtain the intermediate scattering function, $I(q,t)$, for q values of 1.047, 1.396, 1.745, 2.094, 2.443, 3.000, and 3.490 Å^{-1}. It was found that $I(q,t)$ for $q=2.443$, 3.000, and 3.490 Å^{-1} was short ranged. The coordinates produced by MDA were processed to yield $I(q,t)$ obtained from 600 estimates at a set of 16 time points between 0 and 400 time steps ($\simeq1.1\times10^{-12}$ sec) for this set of q values. For 1.047, 1.396, 1.745, and 2.094, $I(q,t)$ is relatively long ranged. The coordinates produced by MDA were processed to obtain 480 estimates of $I(q,t)$ at a set of 27 time points between 0 and 2800 time steps ($\simeq7.7\times10^{-12}$ sec). This was repeated for the coordinates obtained from MDB, and the two sets of estimates of $I(q,t)$ were then averaged. The result is $I(q,t)$ obtained from 960 estimates ranging over a 20000 time-step simulation.

The series II calculations were performed at KFA, Karlsruhe on an IBM3033. For the MD model, 500 krypton atoms were arranged in arbitrary positions in a cubical box of side length $L=36.13$ Å, thus providing a density of 10.6×10^{27} atoms/m^3. The initial distribution of the velocities was chosen according to Maxwell's distribution. To avoid surface effects, periodic boundary conditions were imposed on the system, and the classical Hamilton equations were solved by iteration (time step of 10^{-14} sec). For the pair interaction we chose the potential of Barker *et al.*[3] The cutoff radius r_c for the potential was chosen to be 13.0 Å (3.6σ). We varied r_c and found that cutoff effects are ruled out if $r_c\geq13.0$ Å. The temperature was 295 K. The q values chosen were 0.40, 0.60, 0.80, 1.05, 1.30, 1.55, 1.80, 2.10, 2.40, 2.70, 3.00, 3.25, and 3.50 Å^{-1}. We checked whether the Axilrod-Teller form[4] of the triplet potential u_3 is of importance at the density of 10.6×10^{27} atoms/m^3. We found that effects due to u_3 are distinctly less pronounced than in the case of lower densities (see Refs. 5 and 6).

The series I simulations extended to $\sim7\times10^{-12}$ sec for $q=1.05$ Å^{-1} or to $\sim1.2\times10^{-12}$ sec for $q=3.5$ Å^{-1}, while the series II simulations extended to $\sim2.7\times10^{-12}$ sec for low q and 0.7×10^{-12} sec for high q. The function $I(q,t)$ was set to zero for values higher than these limits and transformed via Eq. (3). This was done by dividing the integrand into 11 intervals and using for each a one-interval 16 point Gaussian integration. The experimental data include a resolution function, which may be approximated by a Gaussian in ω, and which is folded into the scattering function $S(q,\omega)$. This means that $I(q,t)$ should be multiplied by the transform of the resolution function, namely by $R(t)=\exp(-t^2/6.6)$ where t is in 10^{-12} sec units. A second set of transforms were obtained after multiplying by $R(t)$, and this set has the advantage of being smoother because of the damping in t space as well as being directly comparable to the experimental data. For $q=0.4$ Å^{-1} resolution broadening reduces the peak height of $S(q,\omega)$ by $\sim20\%$, while for $q\sim1$ Å^{-1} the reduction is $\sim5\%$ and for $q>2$ Å^{-1} it is negligible. In Figs. 4—7 the resolution broadened data are shown, while Figs. 1—3 show unbroadened data.

III. COMPARISON OF MD RESULTS AND EXPERIMENTAL DATA

The krypton potentials of Aziz[2] and Barker *et al.*[3] are the same for our purposes. In series I we used a lower well depth (170 K in place of 200 K) than given in Refs. 2 and 3 which confirmed the insensitivity (Figs. 1 and 2) of the results on small changes of well depth for $q\geq1$ Å^{-1}. Over the range of q in series I ($1.05\leq q\leq3.5$ Å^{-1}) the structure factors for the two calculations were in good agreement, and from perturbation theory we expect the differences to be significant only for $q<1$ Å^{-1}. For the six q values which are common to the two series, the general agreement of the $I(q,t)$ functions was satisfactory. The quality of this comparison may be illustrated by the comparisons of $S(q,\omega)$ for series I and II shown in Fig. 1. In two of these cases (1.05 and 2.40 Å^{-1}) Fourier oscillations due to truncation in t space are large and limit the usefulness of the comparison, and in the other two cases (2.10 and 3.0 Å^{-1}) the oscillations are small and the comparison is excellent. Truncation effects should become smaller as q is increased because the reduced time range in $I(q,t)$ is easier to cover.

A simple, but informative, quantity is the full width at half maximum (FWHM) amplitude of $S(q,\omega)$ as a function of q, and this is plotted in Fig. 2. We note that the FWHM increases when $\partial S(q)/\partial q$ is negative and levels off when $\partial S(q)/\partial q$ is positive. Where the Fourier oscillations in the MD data lead to large uncertainties in the width there are discrepancies between either neighboring points of the same series or common points of the two series. The dashed line has been drawn through these data to be the best representation of the half-width curve, making allowance for the weighting of different points. A comparison of the uncertainty of these data with that for Fig. 5 of Ref. 1, suggests that similar curves for the hard-sphere fluid and real krypton gas are better known. A comparison of these three cases (the experimental data have been corrected for resolution) is shown in Fig. 3. It is evident that the use of a correct potential in place of the hard-sphere potential improves agreement with experiment in the range $0.4<q<1.6$ Å^{-1}, while for $2.5<q<3.5$ Å^{-1} the agreement appears to worsen. Also we note that the theoretical half-width curve of Bosse *et al.*[7] is similar to our results. Any real differences between the MD curve and the experimental curve should be attributed to the effects of many-body forces. There is some evidence that the half-width of the MD $S(q,\omega)$ is larger than the experimental one for $q\sim1$ and ~3 Å^{-1}, in which case these forces would appear to "slow down" the motions

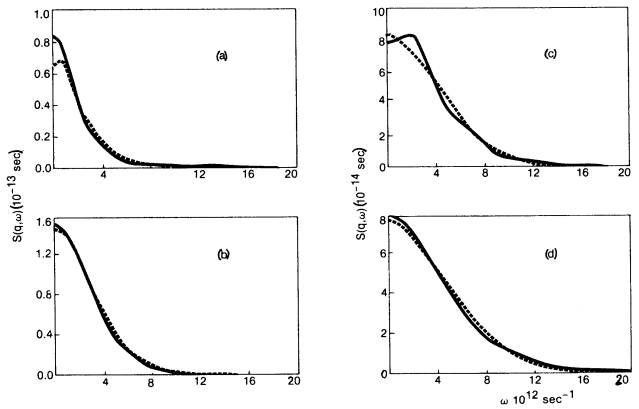

FIG. 1. Comparison of series I and II results for (a) 1.05, (b) 2.1, (c) 2.4, and (d) 3.0 Å^{-1}. The solid line is series II and the dotted line series I.

which contribute to these Fourier components.

The differences between the MD results and experimental data are relatively small, and direct comparisons of $S(q,\omega)$ are perhaps more significant than the summary in Fig. 3. In Figs. 4, 5, and 6 we show this comparison first as a function of ω for fixed q (see Appendix) and then as a function of q for fixed ω. These figures should be compared to Figs. 4 and 8 of Ref. 1. In all cases the resolution broadened data have been used. The lowest value of q in series II ($q=0.4$ Å^{-1}) is approximately 2π divided by half the box size and consequently there may be a larger uncertainty in that case. The overall agreement in Figs. 4 and 5 is satisfactory: at $q=0.4$ Å^{-1} the experimental data have the same half-width but are wider in the wings, at 0.8 Å^{-1} the MD data are appreciably wider, they are a little wider at 1.05 Å^{-1} and in agreement at 1.35 Å^{-1} (which is taken as the average MD data at 1.30 and 1.40 in the two series, respectively). At $q=1.80$ Å^{-1} (Fig. 5) there is excellent agreement, and at the higher q values (2.40, 2.70, and 3.00) the MD data are slightly wider than the experimental data. The central ± 0.5 meV of

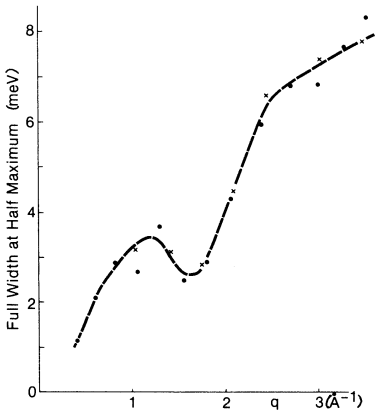

FIG. 2. Full width at half maximum (FWHM) amplitude of $S(q,\omega)$ for the MD calculations. The crosses are series I and the circles are series II, while the dashed line is an approximate curve drawn through the points taking into account their different weightings.

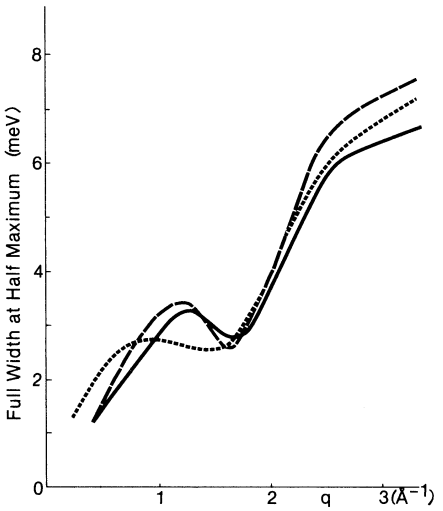

FIG. 3. Comparison of FWHM curve from Fig. 2 and curves for the hard-sphere fluid [dotted line (Ref. 1)] and real krypton [full line (Ref. 1)].

the experimental data, for these last three cases, has been spoiled by Bragg reflections from the pressure vessel and they have been extrapolated to $\omega=0$. Since the area of $I(q,t)$ in the MD work is not well known the central portion of $S(q,\omega)$ is uncertain in the MD data as well. However, all the experimental data have been measured with respect to an absolute scale, so that the comparison for $\hbar\omega > 0.5$ meV is reliable and, for example, the excellent agreement for $q=1.78$ Å^{-1} is striking. It can be seen that the fit of the MD data is worse for 2.7 than 3.0 Å^{-1}, which is due to the effect of Fourier oscillations. A more satisfactory result would be obtained, for example, by averaging these two data sets together.

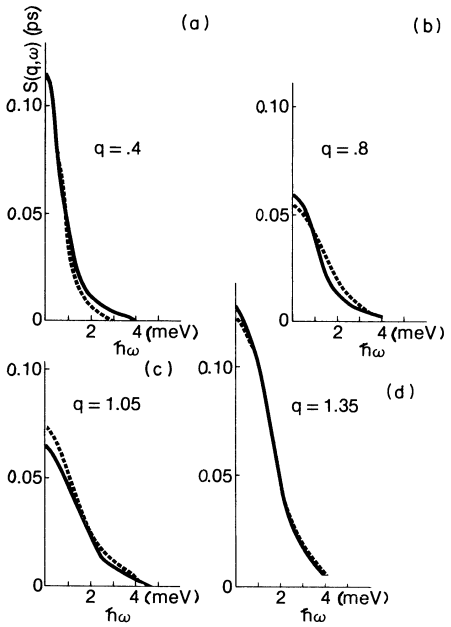

FIG. 4. $S(q,\omega)$ vs ω for fixed q, computer MD data compared to experimental data (Ref. 1): (a) $q=0.4$, (b) 0.8, (c) 1.05, and (d) 1.35 Å^{-1}. The solid line is the experimental and the dotted line is the MD result—(c) and (d) are the average of series I and II. (See Appendix for derivation of experimental data.)

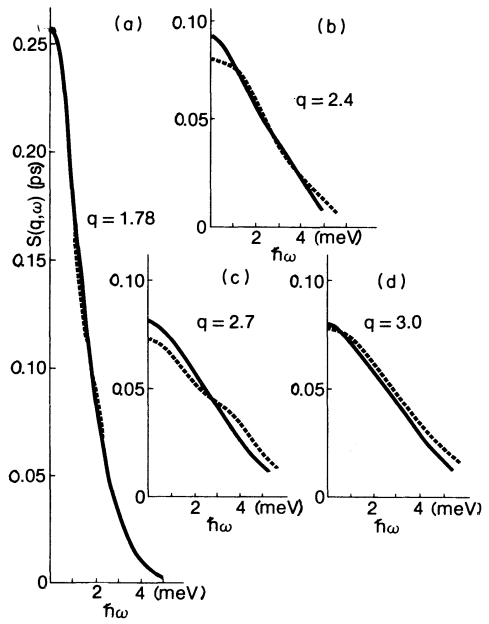

FIG. 5. $S(q,\omega)$ vs ω for fixed q, computer MD data compared to experimental data (Ref. 1): (a) 1.78, (b) 2.4, (c) 2.7, and (d) 3.0 Å^{-1}. The solid lines are experimental and the dotted lines the average of the two MD results (except for 2.7 Å^{-1} which is series II).

In Fig. 6 we show the same data plotted as a function of q for $\omega=0$, 1, 2, and 3 meV in the form $S(q,\omega)/S(q)$. All the MD data are included and the scatter, discussed with respect to Fig. 1, is evident here also. For $\omega=0$ the MD data are lower for $q \geq 2.4$ Å^{-1} confirming that the widths are greater in this region [since $S(q)$ for MD agrees with the experiment for these q's]. At lower q for $\omega=0$ and for $\omega=1$ or 2 meV at all q there is broad agreement within the scatter. However for $\omega=3$ meV, this agreement although striking for $q>1$ Å^{-1} is seen to fail for $q<1$ Å^{-1}. The lower intensity for 3 meV seen in Fig.

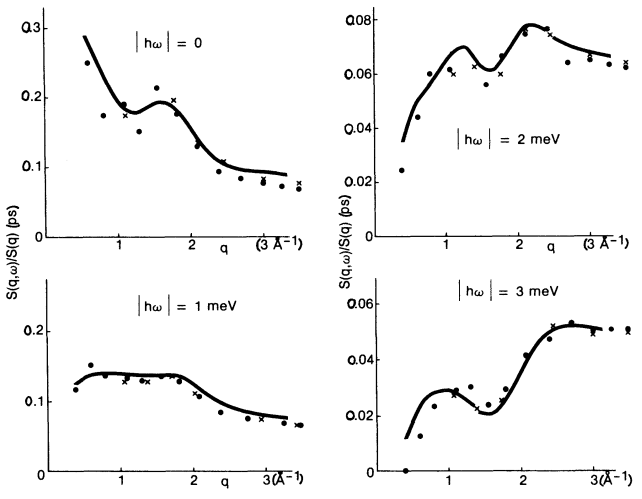

FIG. 6. $S(q,\omega)/S(q)$ vs q for fixed ω, computer MD data compared to experimental data (Ref. 1). The crosses are series I and the circles are series II, and the solid line is a smooth curve drawn through the data in Fig. 8 of Ref. 1 (the q's are measured directly in the constant ω case).

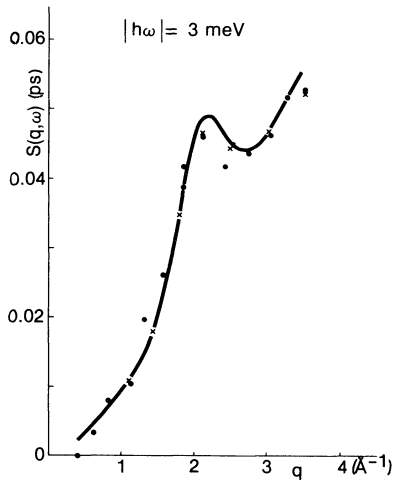

FIG. 7. Dynamic structure factor for an energy transfer of 3 meV. The solid line is the experimental result, and the crosses are series I while the solid circles are series II MD results. Note that a small diffraction peak appears even for $\omega \neq 0$ and that its position is shifted upwards in q relative to the peak in $S(q)$.

4 for $q=0.4$ Å^{-1} is enhanced in the $S(q,\omega)/S(q)$ representation, due to the differences between MD and experimental data for $S(q)$. For this reason the difference extends to higher q. These broader wings may be due to many-body forces, and might indicate that if the experiments and MD calculations were extended to lower q values the onset of side peaks would be more pronounced in the experimental than the MD data. In this event it would be possible to argue that the two effects due to many-body forces (i.e., slowing down of motions observed at high q and intense wings at low q) may be related through the processes which lead to damping or propagation of cooperative modes.

Finally in Fig. 7 we show $S(q,\omega)$ for an energy transfer of 3 meV. The MD data are in good overall agreement with the experimental results and also exhibit a diffraction maximum near 2 Å^{-1} [compared to 1.8 Å^{-1} for $S(q)$]. It seems possible that the experimental and MD peaks do not fit one another, but better data are required to establish a definite result.

IV. CONCLUSIONS

While the MD results are neither as detailed nor as accurate as the neutron scattering data some conclusions may be drawn from these comparisons. First, the use of a fairly realistic potential in place of the hard-sphere potential alters the half-width curve in a direction towards the real curve, showing the importance of the attractive part of the potential. For $q>1$ Å^{-1} a change in well depth by 15% did not produce an observable change, suggesting sensitivity to major changes in the potential only. Some differences with the experimental data remain, which are probably outside the relatively large uncertainties in the MD data (e.g., the greater width of the calculations shown in Fig. 5 at high q and in Fig. 4 for q of 1—0.8 Å^{-1}) and so may be related to the many-body forces. We made a test using the long-range triple-dipole term and found a negligible result in agreement with earlier conclusions.

This suggests that the shorter-ranged many-body terms are producing the discrepancies in Figs. 4 and 5. Such comparisons of $S(q,\omega)$ at fixed q or at fixed ω were used to try to show in detail those regions where a fit occurred and the regions where discrepancies are found. It would be worthwhile to improve and extend the MD data to test these conclusions in greater detail.

The measurements of $S(q)$ reported in Ref. 1 (Fig. 2) showed discrepancies with a simulation using the Barker *et al.*[3] pair potential over similar ranges of q. However, the data did not extend beyond 3 Å^{-1} and it would be worthwhile extending and improving the $S(q)$ work so as to improve this comparison. Meanwhile we conclude that the pair potential approximation gives a good first approximation to $S(q,\omega)$—including $S(q)$—for a dense gas, but that modifications due to shorter-ranged many-body effects can be observed in $S(q)$ and probably in $S(q,\omega)$ over the same regions of q space. These effects appear to increase the width of $S(q,\omega)$ so suggesting a slowing down of the motions leading to these Fourier components.

ACKNOWLEDGMENTS

We are happy to acknowledge the support of the Natural Sciences and Engineering Research Council of Canada, of Cornell University (Ithaca, USA), and of Kernforschungszentrum Karlsruhe (West Germany), for this program. Also we are grateful to Dr. W. Streett for his advice and assistance with the Cornell calculations, and for support from National Science Foundation Grant No. CHE79-09168.

APPENDIX: CONVERSION OF CONSTANT ANGLE NEUTRON DATA TO CONSTANT q DATA

For heavy target atoms, such as krypton, there is a simple procedure for converting the constant angle results of many neutron experiments (e.g., Ref. 1) into constant q results. It is shown in Ref. 1 [Eq. (3)] that for heavy elements the variation of q for constant angle is given by

$$\Delta q_\omega = q_{\text{el}} - q_\omega = -q_{\text{el}}\hbar\omega/4E_0 + \cdots , \tag{A1}$$

where q_{el} and q_ω are the values of q for elastic scattering ($\omega=0$) and for the energy transfer $\hbar\omega$, respectively. The Taylor expansion of $S(q_\omega,\omega)$ is

$$S(q_{\text{el}}-\Delta q_\omega,\omega) = S(q_{\text{el}},\omega) - \Delta q_\omega \left.\frac{\partial S(q,\omega)}{\partial q}\right|_{q=q_{\text{el}}} + \cdots \tag{A2}$$

for a given choice of ω. Now the experimental data at each angle are determined for positive and negative values of ω, and so if we average these values the term in Δq_ω will vanish by virtue of (A1). Thus we obtain

$$S(q_{\text{el}},\omega) = \frac{S(q_\omega;+\omega)+S(q_\omega;-\omega)}{2} + \cdots$$

and this expression was used to obtain the experimental data of Figs. 4 and 5. The q's quoted in these figures are q_{el}.

To obtain constant ω plots, the experimental data are interpolated to the ω required and q_ω is calculated for that value of ω. Each q_ω represents a different angle in this case.

[1]P. A. Egelstaff, W. Gläser, D. Litchinsky, E. Schneider, and J. B. Suck, Phys. Rev. A **27**, 1106 (1983).
[2]R. A. Aziz, Mol. Phys. **38**, 177 (1979).
[3]J. A. Barker, R. O. Watts, J. K. Lee, T. P. Schafer, and Y. T. Lee, J. Chem. Phys. **61**, 3081 (1974).
[4]B. M. Axilrod and E. Teller, J. Chem. Phys. **11**, 229 (1943).
[5]W. Schommers, Phys. Rev. A **22**, 2855 (1980).
[6]W. Schommers, Phys. Rev. A **27**, 2241 (1983).
[7]J. Bosse, E. Leutheusser, and S. Yip, Phys. Rev. A **27**, 1696 (1983).